AMERICAN SCIENTIFIC PUBLISHERS

Science of Advanced Materials
Vol. 14, pp. 1258–1264, 2022
www.aspbs.com/sam

ARTICLE

# Etch Characteristics of Low-K Materials Using $CF_3I/C_4F_8/Ar/O_2$ Inductively Coupled Plasmas

**Jong Woo Hong[1,†], Hyun Woo Tak[1,†], Young Hun Choi[2,3,†], Hee Jung Kim[2,3], Dong Woo Kim[1], and Geun Young Yeom[1,4,*]**

[1] *School of Advanced Materials Science and Engineering, Sungkyunkwan University, Suwon, 16419, South Korea*
[2] *Semiconductor Research & Development (SRD) Center, Samsung Electronics, Hwasung, 18448, South Korea*
[3] *School of Semiconductor Display Engineering, Sungkyunkwan University, Suwon, 16419, South Korea*
[4] *SKKU Advanced Institute of Nano Technology (SAINT), Sungkyunkwan University, Suwon, 16419, South Korea*

## ABSTRACT

In this study, pulsed $CF_3I/C_4F_8/Ar/O_2$ inductively coupled plasmas have been studied for low-k etching, and the effects of $CF_3I$ addition to $C_4F_8/Ar/O_2$ on the plasma characteristics and etch characteristics of low-k materials were investigated. The increased ratio of $CF_3I/(CF_3I+C_4F_8)$ in the gas mixture increased $CF_3$ radicals while decreasing $CF_2$ radicals in the plasma, and which are related to the etching and polymerization, respectively. Therefore, the etch rates of SiCOH increased with increasing the $CF_3I$ ratio. However, the etch selectivity over an amorphous carbon layer and photoresist was the highest at the ratio of 0.5 because the $CF_2$/F flux ratio from the plasma and the C/F ratio on the polymer layer were the highest at the $CF_3I$ ratio of 0.5. The SiCOH damage was decreased with increasing $CF_3I$ ratio and the SiCOH damage appeared to be very low, particularly when the $CF_3I$ ratio was $\geq$0.5 by showing low Si–$CH_3$ bond loss, low F penetration, and a low surface roughness. Therefore, it is believed that, as opposed to the $C_4F_8/Ar/O_2$ gas mixture only, mixing 50% $CF_3I$ into the $C_4F_8/Ar/O_2$ gas mixtures resulted in not only a high etch selectivity over mask materials, but also a potentially reduced etch damage.

**KEYWORDS:** Plasma Etching, Low-K Dielectrics, Hydrogenated Silicon Oxycarbide, Trifluoroiodomethane, Global Warming Potential.

## 1. INTRODUCTION

The critical dimension of semiconductor devices is continuously scaled down to improve the device integration, device performance, profit margins, etc.[1–4] However, due to the reduction of the metal line cross section and the increase in the interconnect length of devices, the interconnect resistance (R) and capacitance (C) tend to increase. Due to the reduction of the metal line cross section and the increase in the interconnect length of devices, the interconnect resistance and capacitance tend to increase. Accordingly, with increasing resistance-capacitance (RC) delay time, chip performance can be degraded. To improve the RC time delay, increases in the interconnection resistance and/or capacitance must be minimized.[5–7] Therefore, low resistivity copper (1.68 $\mu$Ohm.cm) and low permittivity materials (i.e., low-k) are commonly used as interconnect metal and as inter-metal dielectric (IMD), respectively. In general, the IMD currently used in semiconductor devices is SiCOH ($k$-value ~2.7). SiCOH possesses excellent thermal stability, good mechanical stability, and adhesion compared to other low-k materials.[8,9] To preserve the above characteristics and to preserve low-k performances, the minimization of plasma induced damage during the plasma etching of low-k materials such as SiCOH is vital.[10,11] During the plasma etching process, low-k materials are known to be damaged by ultra-violet (UV) photons and F-radicals in fluorocarbon-based plasmas, resulting in an undesirable modification to the chemistry of the carbon containing components within the low-k materials.[12–16] As a result, the RC time delay is increased by the increase in the k value of the dielectric. Furthermore, plasma etching can result in an undercut of the low-k films (occurring under the mask layer) after the removal of plasma damaged sidewall low-k layer during wet cleaning, and which may form voids after metal fill, thereby, affecting overall device reliability. Therefore, a reduction in plasma damage is of utmost importance.

Plasma etching is one of the key processes in the fabrication of integrated circuits. Low-k materials are typically etched using fluorocarbon-based gases, with one

*Author to whom correspondence should be addressed.
Email: gyyeom@skku.edu
†These three authors contributed equally to this work.
Received: 1 May 2022
Accepted: 21 August 2022

frequently used gas being $CF_4$. However, $CF_4$ plasma contains vacuum UV (VUV) photons and high F concentrations. This results in deep penetration of the VUV photons into the low-k material, as well as reactions with F radicals, which leads to both plasma damage and increased surface roughness.[14–16] Decreasing the k value in low-k materials to achieve lower RC time delay tends to cause further damage of low-k materials during $CF_4$ plasma etching due to lower binding energies in the low-k materials as well as more porosity.

To protect low-k materials from plasma induced damage, alternate methods such as UV-assisted curing, cryogenic etching, and post porosity plasma protection, as well as the use of different plasma sources with low or zero VUV emission have been investigated. Unfortunately, these methods are not easily applied to actual device fabrication due to the difficulty in applying to commercial etching systems, low throughput, etc.[17–23] A more productive method is the use of a different fluorocarbon gas chemistry, such as $C_4F_8$, which has been used since years ago for low-k etching of semiconductors instead of $CF_4$. This method effectively suppresses the generation of F radicals in addition to providing higher etch selectivity and an increased vertical profile by using fluorocarbon polymer passivation for nanometer scale etching.[24–26] $CF_3I$ plasma has also been investigated for low-damage etching of low-k materials due to the low VUV emission of the $CF_3I$ plasma in comparison with $CF_4$ plasma. Additionally, the 100-year global warming potential (GWP) of $CF_3I$ is 1, which is extremely small compared to 7,380 for $CF_4$, 14,600 for $CHF_3$ and 10,200 for $C_4F_8$. Recently, semiconductor manufacturers around the world agreed to reduce gas emissions containing high GWPs. This may be achieved by developing new processes using relatively low GWP gases.[27–32]

In this study, the effects of $CF_3I$ addition to $C_4F_8/Ar/O_2$ on the plasma characteristics and etch characteristics (such as etch damage and selectivity) have been investigated using a synchronously pulsed inductively coupled plasma (ICP) etcher, In fact, most of dielectric materials are etched using capacitively coupled plasma (CCP) etch system instead of ICP etch system in the industry due to the higher etch selectivity over mask layers but, in this study, the ICP etch system was used to etch low-k dielectric materials together with a synchronized pulsing to investigate the possibility for improved etch selectivity similar to the CCP etch system in addition to the improved low-k damage, etc. $CF_3I$ is a low-polymerizing etching gas, while $C_4F_8$ is a high-polymerizing gas. It is believed that the polymerization rate can be controlled by mixing low- and high-polymerizing gases in the correct proportion, leading to improved etching selectivity and reduced etching damage. Compared to continuous wave (CW) plasma, pulsed plasmas have low average electron energies and can more effectively control plasma characteristics, therefore, pulse plasma was used in this study to improve etch characteristics.

## 2. EXPERIMENTAL DETAILS

A schematic drawing of the pulsed ICP plasma reactor used in the experiment is shown in Figure 1. A 27.12 MHz radio frequency (RF) pulsed source power (ENI RF Amplifiers, A-1000) was supplied to an ICP antenna using a silver-coated two-turn Cu coil to sustain the plasma, while 13.56 MHz RF pulsed power (SEREN, R10001) was applied to the bottom electrode for substrate biasing. In our experimental condition, even though 27.12 MHz RF power which is a harmonic frequency of 13.56 MHz bias power was used for the ICP source power, no noticeable interference between two RF powers was observed. Both the source power and the bias power were pulsed with a 50% duty cycle at 1 kHz frequency and were synchronized through a digital delay generator (DG645, Stanford Research Systems), which allows synchronous pulsing of the source power and bias power. The water cooled 300 mm diameter substrate holder was located 20 cm below the antenna. Processing gases ($CF_3I/C_4F_8/Ar/O_2$) were injected through 1 mm diameter holes installed beneath the 2 cm thick $Al_2O_3$ dielectric window located below the ICP antenna.

300 nm thick SiOCH blanket films ($k$ value of 2.7) deposited by plasma enhance chemical vapor deposition using tetramethylcyclote-trasiloxane (TMCTS) which have a porositiy of about 30% with an average pore size below 2.5 nm on silicon wafers were used as the low-k samples. A 500 nm thick amorphous carbon layer (ACL)

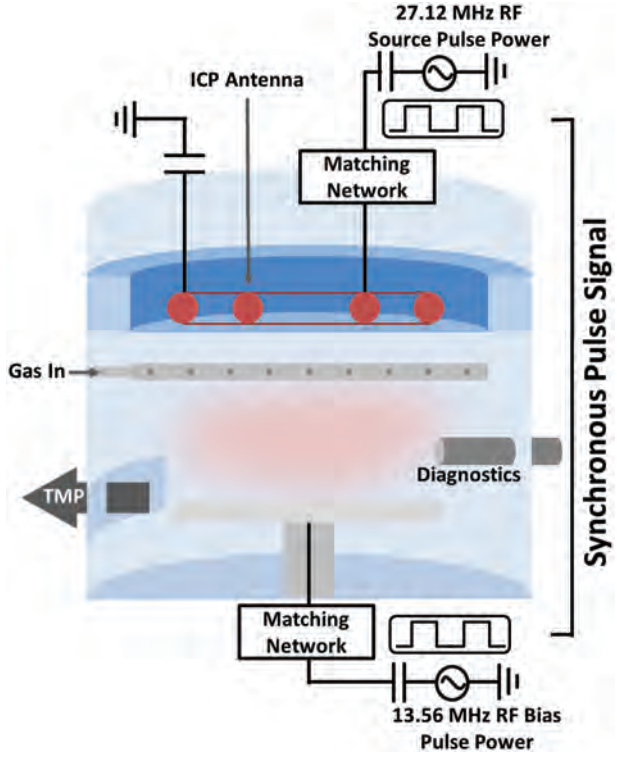


**Fig. 1.** A schematic drawing of the synchronously pulsed ICP etch system used in this study.



ARTICLE

and a 1300 nm thick photoresist (PR) layer were used as mask materials. The SiOCH, ACL, and PR layers were etched with varying ratios of $CF_3I/C_4F_8$ while maintaining a total flow rate of 120 sccm for $CF_3I/C_4F_8$/Ar (40 sccm)/$O_2$ (20 sccm) and the total pressure was kept at 1.3 Pa (10 mTorr) using an automatic pressure controller. To study etch rates and etch selectivities between the SiCOH and mask materials, the pulsed 27.12 MHz ICP source power and the pulsed 13.56 MHz bias power were kept at 200 W and −170 V DC self-bias voltage (ICP power is the power during the plasma-on time and the bias voltage is the time averaged bias voltage), respectively, while maintaining a pulse frequency of 1 kHz (pulse period 1000 $\mu$s) and 50% duty percentage.

The plasmas generated with $CF_3I/C_4F_8/Ar/O_2$ gas mixtures were introduced into the quadrupole mass spectrometer (QMS, PSM003, Hiden Analytical) via an orifice of 100 $\mu$m in diameter located at the sidewall of the vacuum chamber, and the m/z to the wall was measured with an energy resolution of 0.05 eV. The mass spectrometer was operated in the positive ion detection mode (no pass energy for positive ion detection was chosen and no calibration of mass dependency was made). The optical emissions from the radicals, which dominantly affect the etching, were also observed using optical emission spectroscopy (OES, Andoristar734) from 270 to 800 nm with a time averaged mode. An exposure time of 0.1 s and 10 accumulations were used in all of the experiments. Optical emission peak intensities were observed at 270–300, 321, 342, 500–600, 519, 704, and 750 nm, which are related to the emissions from $CF_2$, CFI, $CF_3$, I, F, and Ar, respectively.[33] For surface analysis of the etched SiCOH films, X-ray photoelectron spectroscopy (XPS, ThermoFisher Scientific, K-Alpha+) was used and the depth profiles of C 1 s, F 1 s, etc. were carried out by sputter-etching using an $Ar^+$ ion gun every 10 s after each XPS measurement in the XPS chamber. For X-ray intensity for the XPS, we kept the same condition and the 5 samples were loaded at the same time in the XPS chamber and analyzed in sequence. A Mg K$\alpha$ twin-anode source with an X-ray incident angle of 0° was used for the XPS measurements. To examine the chemical modification of the SiCOH film after the etching, the Fourier transform infrared spectra (FT–IR, Bruker Hyperion3000) of the films were measured in the range from 2000 to 400 $cm^{-1}$. In the FT-IR, a purge system was installed on the microscope stage to reduce spectral interference from infrared-absorbing atmospheric gases such as water and $CO_2$. Also, even though, most of researchers use the absorbance curve for FT-IR, the transmittance curve was used because it appeared to show the variation more distinctively for our experimental data. The FT–IR spectra give relative information about bond concentrations within the film and were used to observe relative changes in Si–$CH_3$ bonds (1270–1280 $cm^{-1}$) in the etched SiCOH films. For the measurements of root mean square (RMS) surface roughness, XPS, and FTIR of etched SiCOH films, a fixed etch depth of ~150 nm was used while a fixed time was used for the measurements of etch rates, etch selectivities, and plasma characteristics.

## 3. RESULTS AND DISCUSSION

Figures 2(a) and (b) show the etch rates of SiCOH, PR and the ACL and etch selectivities of SiCOH over PR and ACL, respectively. These were measured as a function of the ratio of $CF_3I/(CF_3I+C_4F_8)$ at a flow rate of $CF_3I+C_4F_8 = 60$ sccm in the $CF_3I/C_4F_8/Ar/O_2$ gas mixture and at 1.3 Pa (10 mTorr) operating pressure. Flow rates of $Ar/O_2$ were also maintained at 40 sccm/20 sccm, and which were determined to be optimized flow rates from previous experiments. For etching, 200 W of 27.12 MHz RF power was applied to the ICP source and −170 V of DC self-bias voltage was used for substrate biasing using 13.56 MHz RF power. The ICP source power and bias power were synchronized at 1 kHz with 50% duty

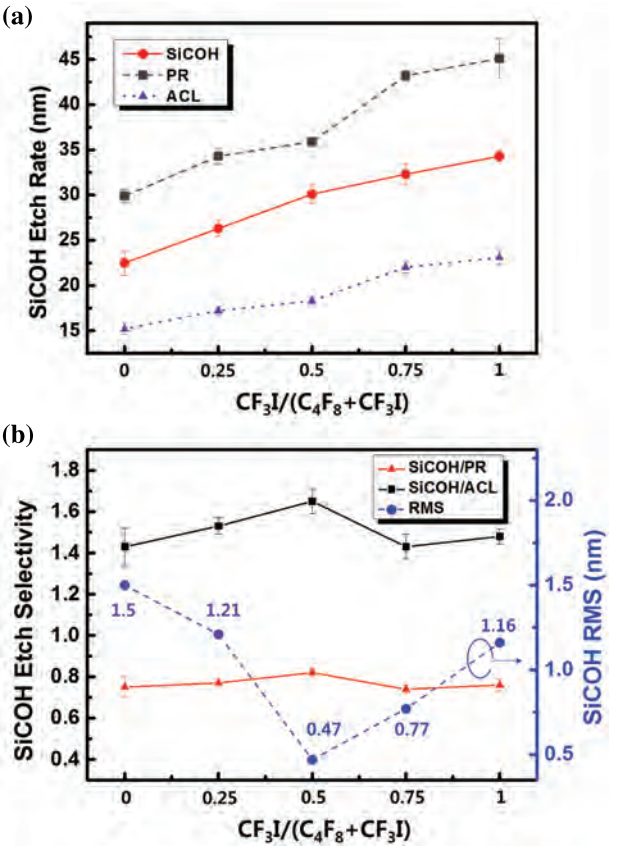


**Fig. 2.** (a) Etch rates of SiCOH, ACL, and PR in $CF_3I/C_4F_8/Ar/O_2$ synchronous pulsed plasmas as a function of $CF_3I/(CF_3I+C_4F_8)$ ratio. (b) Etch selectivity for SiCOH/ACL and SiCOH/PR, and RMS surface roughness of etched SiCOH surfaces. The operating parameters: Pressure 1.3 Pa (10 mTorr), Ar 40 sccm, $O_2$ 20 sccm, $(CF_3I+C_4F_8)$ 60 sccm, 200 W 27.12 MHz ICP source power, −170 V DC self-bias voltage using 13.56 MHz, 1 kHz pulse frequency, duty ratio 50%, and synchronized pulsing.

percentage. As shown in Figure 2(a), an increase in the ratio of $CF_3I/(CF_3I+C_4F_8)$ led to a nearly linear increase in etch rates of SiCOH, PR, and ACL. Therefore, the highest etch rates were observed at 100% $CF_3I$ while the lowest etch rates were observed at 100% $C_4F_8$. On the contrary, as shown in the Figure 2(b), the improvements in etch selectivities for SiCOH/PR and SiCOH/ACL at the ratio of $CF_3I/(C_4F_8+CF_3I)$ of 0.5 from ~1.43 ($CF_3I=0$) to ~1.65 and from ~0.75 ($CF_3I=0$) to ~0.82, respectively, were observed. Figure 2(b) also shows the AFM surface roughness on the etched SiCOH measured for different $CF_3I/(C_4F_8+CF_3I)$ ratios and, as shown in the figure, the lowest RMS surface roughness of 0.47 nm was observed at the ratio of 0.5 (the RMS surface roughness of unetched SiCOH was 0.31 nm).

Using quadrupole mass spectrometry, the species dissociated in the plasma were investigated as a function of the ratio of $CF_3I/(CF_3I+C_4F_8)$ in the $CF_3I/C_4F_8/Ar/O_2$ gas mixtures using the process conditions shown in Figure 2 and the results are shown in Figure 3. To measure the species in the plasma without further dissociation of formed radicals, the positive ion mode was used, and therefore, the positive ions formed in the plasma were measured directly in the mass spectrometer. As shown in Figure 3, when 100% $C_4F_8$ was used (i), various fluorocarbon species such as CF, $CF_2$, and $C_xF_y$, which cause polymerization on the surface, could be observed and as the $CF_3I$ is increased to 100%; on the other hands (v), the $CF_3$, $CF_2I$, $I_2$, etc., which are not quite related to the polymerization of the substrate surface, increased while decreasing the species causing polymerization. The low concentration of polymerization species, including $CF_2$ in $CF_3I$ plasma, is believed to be related to the dissociation of $CF_3I$ primarily into $CF_3$ and I as a result of the low bonding energy between C and I in $CF_3I$ (C–I bond (2.4 eV) < C=C bond (2.8 eV) < C–C (4.3 eV) < C–F bond (5.6 eV)). In mass spectrometry, no noticeable fluorine peak intensity was observed, possibly due to insufficient positive $F^+$ ion formation in the plasma.

To understand more about the dissociated species generated using the $CF_3I/C_4F_8/Ar/O_2$ gas mixtures, optical emission intensities were measured by OES for the process conditions shown in Figure 2. The results for different ratios of $CF_3I/(CF_3I+C_4F_8)$ in the $CF_3I/C_4F_8/Ar/O_2$ gas mixtures are shown in Figure 4(a). As shown in Figure 4(a), optical emission intensities from F and Ar were measured at 704 and 750 nm, respectively. Additionally, sharp line emissions from $CF_2$ and $CF_3$ were observed as band emissions at 270–430 nm and 510–600 nm, respectively. Also, with an increase in $CF_3I$ in the gas mixture, I related peaks such as $CF_xI$, $I_2$, and I were observed at 321, 342, and 519 nm, respectively. The optical emission intensities of $CF_2$, $CF_3$, I and F observed in the Figure 4(a) and the ratios of $CF_2/F$ and $CF_3/F$ were measured. The results are shown in Figure 4(b). In Figure 4(b), the increase in $CF_3I$ in the ratios of $CF_3I/(CF_3I+C_4F_8)$ led to the increased optical emission intensities from I, $CF_3$, and $CF_xI$, while decreasing the optical emission intensities from $CF_2$ and F. Therefore, similar to quadrupole mass spectrometry, as the amount of $CF_3I$ in the plasma is increased, a possibility in the increase of $+CF_3$ with a decrease of $CF_2$ in the plasma was observed. While

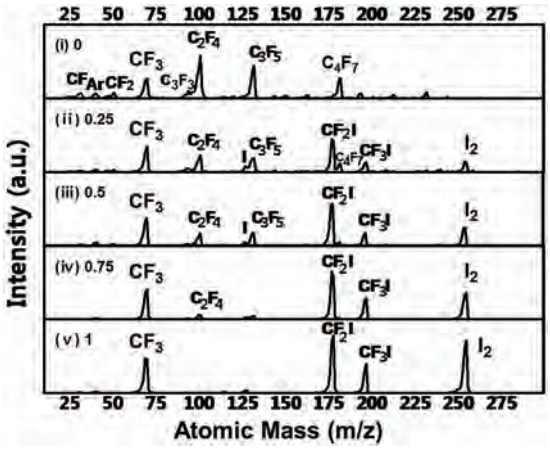


**Fig. 3.** Quadruple mass spectrometry data of positive ions detected in $CF_3I/C_4F_8/Ar/O_2$ synchronous pulsed plasmas as a function of $CF_3I/(CF_3I+C_4F_8)$ ratio. The species dissociated in the plasma were investigated under the process conditions listed in Figure 2.

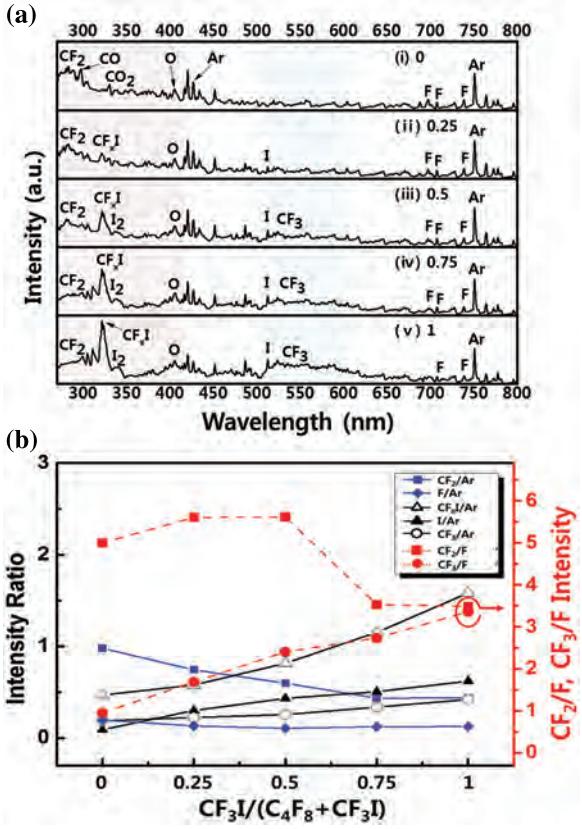


**Fig. 4.** (a) OES data of $CF_3I/C_4F_8/Ar/O_2$ synchronously pulsed plasmas as a function of $CF_3I/(CF_3I+C_4F_8)$ ratio for the process conditions in Figure 2. (b) Optical emission intensity of $CF_2$, $CF_3$, F, CFI, and I, and the ratios of $CF_2/F$ and $CF_3/F$.



ARTICLE

$CF_3$/F continues to increase, it is particularly clear that for $CF_3$/F and $CF_2$/F, the highest $CF_2$/F level (that is, the highest amount of polymerization species/etch species) was observed at a 0.5 ratio of $CF_3I/(CF_3I+C_4F_8)$. This may be related to the highest etch selectivity observed at the ratio of 0.5 in Figure 2(b). Also, the similar etch selectivities for 100% $C_4F_8$ and 100% $CF_3I$ in Figure 2(b) could be related to the similar ratio of $CF_2$/F.

The surfaces of the SiCOH materials etched using different ratios of $CF_3I/(CF_3I+C_4F_8)$ in the $CF_3I/C_4F_8/Ar/O_2$ gas mixtures were investigated by XPS. Figures 5(a) and (b) show XPS narrow scan data of C 1 s and F 1 s observed on the etched SiCOH surfaces, respectively. The surface of SiCOH was observed after a 10 s sputter with $Ar^+$ ions to remove the oxide formed during the exposure to air. As shown in Figures 5(a) and (b), the peak intensities of carbon and fluorine decreased with an increase in the $CF_3I$ ratio in the $CF_3I/C_4F_8/Ar/O_2$ gas mixtures. However, the carbon peak intensity decreased significantly when the ratio of $CF_3I/(C_4F_8+CF_3I)$ was greater than 0.5, while the fluorine intensity decreased continuously with an increase in $CF_3I$ in the gas mixture. Figure 5(c) shows the C/F ratios in addition to the atomic composition of species observed on the etched SiCOH surfaces for different $CF_3I/(CF_3I+C_4F_8)$ ratios. As shown in Figure 5(c), despite a decrease in both carbon and fluorine with the increase of the $CF_3I/(CF_3I+C_4F_8)$ ratio, the ratio of C/F on the etched SiCOH surface was the highest at a 0.5 $CF_3I$ ratio. This may be attributed to the high $CF_2$/F ratio contained in the plasma, as observed in Figure 4(b). Using $Ar^+$ ion depth profiling, the thickness of the fluorocarbon polymer layer on the etched SiCOH surface was investigated by measuring the change in atomic percentages for carbon and fluorine. Results are shown in Figure 5(d), where the thickness of the fluorocarbon polymer layer decreased continuously with an increase in the $CF_3I$ ratio, and, from the $CF_3I$ ratio of 0.75, nearly no fluorocarbon polymer layer was observed on the etched SiCOH surface. Therefore, with increasing $CF_3I$ ratio, the thickness of the fluorocarbon polymer layer on SiCOH decreased while the C/F ratio in the polymer layer was the highest at the $CF_3I$ ratio of 0.5. Also, at the $CF_3I$ ratio of 0.5, the lowest RMS surface roughness was observed as shown in Figure 2(b). This is believed to be related to the high $CF_2$/F flux ratio from the plasma and the high C/F ratio in the polymer layer at the ratio of 0.5. Figure 5(d) also shows the degree of F radical penetration into the remaining SiCOH layer (the layer with ~20% carbon) under the fluorocarbon polymer layer and, as shown in Figure 5(d), significant penetration of F radicals into the remaining SiCOH layer could be observed for

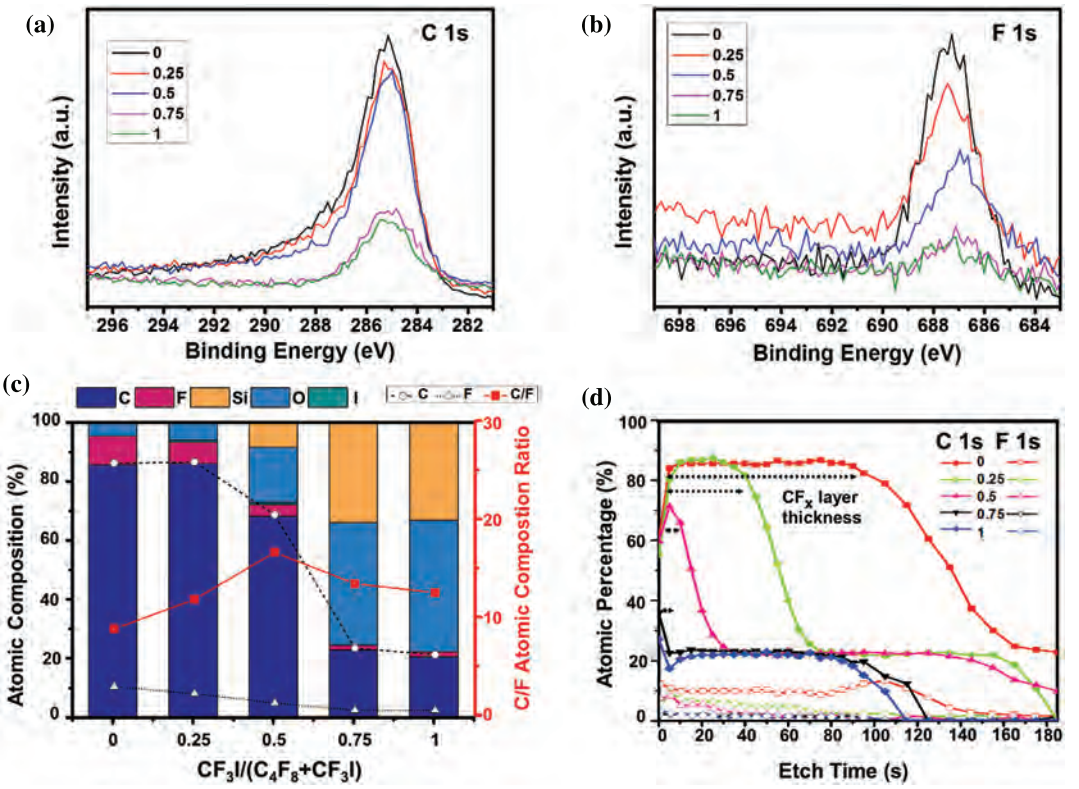


**Fig. 5.** XPS surface analysis of the SiCOH material etched using varying ratios of $CF_3I/(CF_3I+C_4F_8)$ in the $CF_3I/C_4F_8/Ar/O_2$ gas mixtures. (a) and (b) Show XPS narrow scan data for C 1 s and F 1 s observed on the etched SiCOH surfaces, respectively. (c) shows the C/F ratios in addition to the atomic composition of species observed on the etched SiCOH surfaces for different $CF_3I/(CF_3I+C_4F_8)$ ratios. (d) $Ar^+$ ion depth profiling data showing the thickness of the fluorocarbon polymer layer on the etched SiCOH surfaces by measuring the change of atomic percentages for carbon and fluorine in the etched SiCOH.

$CF_3I$ ratios from 0 to 0.25. However, no significant penetration of F into the SiCOH layer was observed when the ratio was higher than 0.5, indicating a reduction in SiCOH damage due to etching with the $CF_3I$ ratio $\geq$0.5.

Using FT–IR, the surface damage to the etched SiCOH for different ratios of $CF_3I/(C_4F_8+CF_3I)$ was further investigated. It has been shown that when low-k materials are damaged by VUV radiation, the Si–$CH_3$ bonds in the material are broken and replaced by Si–OH during a reaction with the hydroxyl ions. This increases the dielectric constant, $k$ values.[34–37] Therefore, using FT–IR to examine Si–$CH_3$ bonds at 1270 $cm^{-1}$, changes in peak intensity in the SiCOH layer etched with the varying ratios of $CF_3I$ were investigated. Figure 6 shows the FT–IR data for unetched SiCOH, as well as SiCOH etched with varying ratios of $CF_3I/(CF_3I+C_4F_8)$. Blanket etched/unetched SiCOH samples not patterned samples were used for the FT-IR measurement. (Due to the difficulty in the FT-IR measurement with patterned SiCOH samples, the blanket samples were used for FT-IR measurement, but, the characteristics of sidewall SiCOH for patterned samples could be different from the blanket samples) As shown in Figure 6, the peak intensity related to Si–$CH_3$ bonds could be observed for the unetched reference SiCOH (vi), while no noticeable peak intensity was observed for SiCOH etched with the $CF_3I$ ratio of 0 (i) (that is, for etching with $C_4F_8$). However, with an increase in the $CF_3I$ ratio (i$\rightarrow$v), the peak intensity increased and, as shown in the inset figure of Figure 6, the peak intensity of the Si–$CH_3$ bonds (Si–$CH_3$ stretching mode at 1270 $cm^{-1}$) increased significantly at a ratio of 0.5, and remained high up to a ratio of 1.0. Even though the change in the peak intensity of Si–$CH_3$ bonds does not necessarily indicates the change in the SiCOH damage status, this may be related to the SiCOH damage. And, the increase of the peak intensity of the Si–$CH_3$ bonds for $CF_3I \geq 0.5$ might indicate that the damage to the SiCOH could be relatively insignificant when the $CF_3I$ ratio was $\geq$0.5.

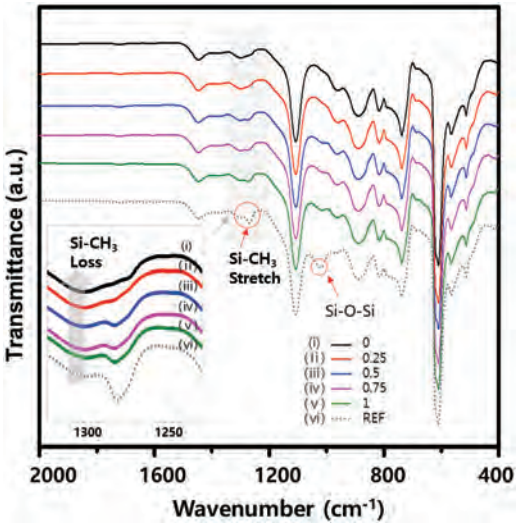


**Fig. 6.** FT–IR transmittance spectra of unetched SiCOH, as well as SiCOH etched with varying ratios of $CF_3I/(CF_3I+C_4F_8)$. Inset figure shows a magnified FT–IR section for the wavelength from 1270–1280 $cm^{-1}$.

## 4. CONCLUSIONS

The effects of the $CF_3I/(CF_3I+C_4F_8)$ ratio on the etch characteristics, plasma characteristics, and etch damage by the synchronized pulsed ICP etching (50% duty percentage with 1 kHz pulse frequency) of SiCOH using $CF_3I/C_4F_8/Ar/O_2$ gas mixtures were investigated. With an increase in the $CF_3I$ ratio, $CF_3$ radicals increase, while $CF_2$ radicals decrease. Therefore, the etch rates increase with $CF_3I$ ratio as the polymer layer thickness decreases on the etched SiCOH material. However, etch selectivity was the highest and surface roughness was the lowest at a ratio of 0.5. This occurs because the $CF_2$/F flux ratio from the plasma and the C/F ratio of the fluorocarbon layer on the etched SiCOH surface were the highest at a $CF_3I$ ratio of 0.5, despite a continuous decrease in the polymer layer with an increase in the $CF_3I$ ratio. The SiCOH damage occurred due to the etching was estimated by F radical penetration depth and Si–$CH_3$ bond loss (caused by VUV radiation) and appears to decrease with an increase in the plasma $CF_3I$ ratio. This is particularly evident when the $CF_3I$ ratio is $\geq$0.5 and it is possibly related to the quality of the polymer layer with the high C/F ratios for $CF_3I \geq$ 0.5 formed on the SiCOH surface in addition to F penetration into the SiCOH layer. Therefore, it can be concluded that, by using a gas mixture containing 50% $CF_3I$ and 50% $C_4F_8$, as opposed to 100% $C_4F_8$, not only improvements in etch selectivity, but also a decrease in etch damage might be expected during the etching of low-k materials.

### Conflicts of Interest

The authors declare no conflicts of interest.

**Acknowledgments:** This work was supported by the Korea Institute of Energy Technology Evaluation and Planning (KETEP) and the Ministry of Trade, Industry & Energy (MOTIE) of the Republic of Korea (No. 20202010100020).

## References and Notes

1. S. E. Thompson and S. Parthasarathy, Moore's law: The future of Si microelectronics. *Mater. Today* 9, 20 (**2006**).
2. T. H. Bao, J. Ryckaert, Z. Tokei, A. Mercha, D. Verkest, A. V. Y. Thean, and P. Wambacq, Statistical timing analysis considering device and interconnect variability for BEOL requirements in the 5-nm node and beyond. *IEEE Transactions on VLSI Systems* 25, 1669 (**2017**).
3. S. Lee, J. Woo, D. Jung, J. Yang, J.-H. Boo, H. Kim, and H. Chae, Effect of etching on dielectric constant and surface composition of SiCOH low-k films in inductively coupled fluorocarbon plasmas. *Thin Solid Films* 517, 3942 (**2009**).



ARTICLE

4. D. Shamiryan, M. R. Baklanov, S. Vanhaelemeersch, and K. Maex, Comparative study of SiOCH low-k films with varied porosity interacting with etching and cleaning plasma. *J. Vac. Sci. Technol., B* 20, 1923 (**2002**).
5. Y.-L. Cheng, J.-F. Huang, Y.-M. Chang, and J. Leu, Impact of plasma treatment on structure and electrical properties of porous low dielectric constant SiCOH material. *Thin Solid Films* 544, 537 (**2013**).
6. M. Nagai, T. Hayashi, M. Hori, and H. Okamoto, Low-k SiOCH film etching process and Its diagnostics employing $Ar/C_5F_{10}O/N_2$ plasma. *Japanese Journal of Applied Physics* 45, 7100 (**2006**).
7. M. R. Baklanov, J.-F. Marneffe, D. de Shamiryan, A. M. Urbanowicz, H. Shi, T. V. Rakhimova, H. Huang, and P. S. Ho, Plasma processing of low-k dielectrics. *J. Appl. Phys.* 113, 4 (**2013**).
8. K. Laer, S. Van Tinck, V. Samara, J. Marneffe, and A. De Bogaerts, Etching of low-k materials for microelectronics applications by means of a $N_2/H_2$ plasma: Modeling and experimental investigation. *Plasma Sources Science Technology* 22, 025011 (**2013**).
9. C. Ye, Y. Xu, X. Huang, Z. Xing, J. Yuan, and Z. Ning, Effect of low-frequency power on etching of SiCOH low-k films in $CHF_3$ 13.56 MHz/2 MHz dual-frequency capacitively coupled plasma. *Microelectron. Eng.* 86, 421 (**2009**).
10. T. Yamaguchi, T. Komuro, C. Koshimizu, S. Takashima, K. Takeda, H. Kondo, K. Ishikawa, M. Sekine, and M. Hori, Direct current superposed dual-frequency capacitively coupled plasmas in selective etching of SiOCH over SiC. *J. Phys. D: Appl. Phys.* 45, 025203 (**2011**).
11. J. Lee and D. Graves, The effect of VUV radiation from $Ar/O_2$ plasmas on low-k SiOCH films. *J. Phys. D: Appl. Phys.* 44, 325203 (**2011**).
12. Z. Otell, V. Šamara, A. Zotovich, T. Hansen, J.-F. Marneffe, and M. R. Baklanov, Vacuum ultra-violet emission of $CF_4$ and $CF_3I$ containing plasmas and their effect on low-k materials. *J. Phys. D: Appl. Phys.* 48, 395202 (**2015**).
13. H. Zheng, E. T. Ryan, Y. Nishi, and J. L. Shohet, Effect of vacuum-ultraviolet irradiation on the dielectric constant of low-k organosilicate dielectrics. *Appl. Phys. Lett.* 105, 202902 (**2014**).
14. D. V. Lopaev, S. M. Zyryanov, A. I. Zotovich, T. V. Rakhimova, Y. A. Mankelevich, A. T. Rakhimov, and M. R. Baklanov, Synergistic effect of VUV photons and F atoms on damage and etching of porous organosilicate films. *Plasma Process and Polymers* 15, 1700213 (**2018**).
15. T. V. Rakhimova, D. V. Lopaev, Y. A. Mankelevich, A. T. Rakhimov, S. M. Zyryanov, K. A. Kurchikov, N. N. Novikova, and M. R. Baklanov, Interaction of F atoms with SiOCH ultra-low-k films: I. *Fluorination and Damage. Journal of Physics D* 48, 175203 (**2015**).
16. B. Jinnai, S. Fukuda, H. Ohtake, and S. Samukawa, Prediction of UV spectra and UV-radiation damage in actual plasma etching processes using on-wafer monitoring technique. *J. Appl. Phys.* 107, 043302 (**2016**).
17. T. Frot, W. Volksen, T. Magbitang, D. Miller, S. Purushothaman, M. Lofaro, R. Bruce, and G. Dubois, Mitigation of plasma-induced damage in porous low-k dielectrics by cryogenic precursor condensation. *Journal of Physics D* 49, 175203 (**2011**).
18. T. Frot, W. Volksen, T. Magbitang, D. Miller, S. Purushothaman, M. Lofaro, R. Bruce, and G. Dubois, Post porosity plasma protection a new approach to integrate $k \leq 2.2$ porous ULK materials, *IEEE International Interconnect Technology Conference* 5940272 (**2011**).
19. T. Rakhimova, A. Rakhimov, Y. A. Mankelevich, D. Lopaev, A. Kovalev, A. Vasil'eva, S. Zyryanov, K. Kurchikov, O. Proshina, and D. Voloshin, Low-k films modification under EUV and VUV radiation. *Journal of Physics D* 47, 025102 (**2014**).
20. L. Zhang, R. Ljazouli, P. Lefaucheux, T. Tillocher, R. Dussart, Y. A. Mankelevich, J.-F. Marneffe, S. De Gendt, and M. R. De Baklanov, Low damage cryogenic etching of porous organosilicate low-k materials using $SF_6/O_2/SiF_4$. *ECS Journal of Solid State Science and Technology* 2, N131 (**2013**).
21. R. Dussart, T. Tillocher, P. Lefaucheux, and M. Boufnichel, Plasma cryogenic etching of silicon: From the early days to today's advanced technologies. *Journal of Physics D* 47, 123001 (**2014**).
22. V. Jousseaume, L. Favennec, A. Zenasni, and G. Passemard, Plasma-enhanced-chemical-vapor-deposited ultralow k for a postintegration porogen removal approach. *Appl. Phys. Lett.* 88, 182908 (**2006**).
23. V. Raballand, G. Cartry, and C. Cardinaud, Porous SiOCH, SiCH and $SiO_2$ etching in high density fluorocarbon plasma with a pulsed bias. *Plasma Process and Polymers* 4, 563 (**2007**).
24. I. Reid and G. Hughes, Investigation of varying $C_4F_8/O_2$ gas ratios on the plasma etching of carbon doped ultra-low-k dielectric layers. *Semicond. Sci. Technol.* 22, 636 (**2007**).
25. G. Kokkoris, A. Goodyear, M. Cooke, and E. Gogolides, A global model for $C_4F_8$ plasmas coupling gas phase and wall surface reaction kinetics. *Journal of Physics D* 41, 195211 (**2008**).
26. S. Tachi, Impact of plasma processing on integrated circuit technology migration: From 1 $\mu$m to 100 nm and beyond. *Journal of Vacuum Science and Technology A* 21, S131 (**2003**).
27. R. Levy, V. Zaitsev, K. Aryusook, C. Ravindranath, V. Sigal, A. Misra, S. Kesari, D. Rufin, J. Sees, and L. Hall, Investigation of $CF_3I$ as an environmentally benign dielectric etchant. *Journal of Materials Research and Technology* 13, 2643 (**1998**).
28. E. Soda, S. Kondo, S. Saito, Y. Ichihashi, A. Sato, H. Ohtake, and S. Samukawa, Low-damage low-k etching with an environmentally friendly $CF_3I$ plasma. *J. Vac. Sci. Technol., A* 26, 875 (**2008**).
29. S. Samukawa, Y. Ichihashi, H. Ohtake, E. Soda, and S. Saito, Environmentally harmonized $CF_3I$ plasma for low-damage and highly selective low-k etching. *J. Appl. Phys.* 103, 053310 (**2008**).
30. H. Ohtake, H. Ishihara, T. Fuse, A. Koshiishi, and S. Samukawa, Highly selective and high rate $SiO_2$ etching using argon-added $C_2F_4/CF_3I$ plasma. *J. Vac. Sci. Technol., B* 21, 2142 (**2003**).
31. O. V. Proshina, T. V. Rakhimova, D. V. Lopaev, V. Samara, M. R. Baklanov, and J. F. Marneffe, Experimental and theorerical study of RF capacitively coupled plasma in $Ar–CF_4–CF_3I$ mixtures. *Plasma Sources Sci. Technol.* 24, 055006 (**2015**).
32. A. Zotovich, O. Proshina, Z. Otell, D. Lopaev, T. Rakhimova, A. Rakhimov, J. F. Marneffe, and M. R. Baklanov, Comparison of vacuum ultra-violet emission of $Ar/CF_4$ and $Ar/CF_3I$ capacitively coupled plasmas. *Plasma Sources Sci. Technol.* 25, 055001 (**2016**).
33. J. W. Coburn and M. Chen, Optical emission spectroscopy of reactive plasmas: A method for correlating emission intensities to reactive particle density. *J. Appl. Phys.* 51, 3134 (**1980**).
34. X. Guo, J. Jakes, S. Banna, Y. Nishi, and J. Shohet, Effects of plasma and vacuum-ultraviolet exposure on the mechanical properties of low-k porous organosilicate glass. *J. Appl. Phys.* 116, 044103 (**2014**).
35. J. Bao, H. Shi, H. Huang, P. S. Ho, M. D. Goodner, M. Moinpour, and G. M. Kloster, Mechanistic study of plasma damage of low k dielectric surfaces. *J. Vac. Sci. Technol., B* 26, 219 (**2008**).
36. M. Lepinay, D. Lee, R. Scarazzini, M. Bardet, M. Veillerot, L. Broussous, C. Licitra, V. Jousseaume, F. Bertin, V. Rouessac, and A. Ayral, Impact of plasma reactive ion etching on low dielectric constant porous organosilicate films' microstructure and chemical composition. *Microporous Mesoporous Mater.* 228, 297 (**2016**).
37. S. Yasuhara, J. Chung, K. Tajima, H. Yano, S. Kadomura, M. Yoshimaru, N. Matsunaga, T. Kubota, H. Ohtake, and S. Samukawa, Structure-designable method to form super low-k SiOC film ($k = 2.2$) by neutral-beam-enhanced chemical vapour deposition. *Journal of Physics D* 42, 055208 (**2009**).